Multi-peak single object emission of $MAPbBr_3$ nanoplatelets synthesised using a non-template ligand-assisted reprecipitation route

Suhaas Gupta[1*], Dmytro Vorontsov[2], Anna Fučíková[2], František Trojánek[2], Dominika Zákutná[3,4], Jozef Veselý[5], Petr Harcuba[5], Milan Dopita[1]

[1] Department of Condensed Matter Physics, Faculty of Mathematics and Physics, Charles University, Ke Karlovu 5, 12116 Prague 2, Czech Republic
[2] Department of Chemical Physics and Optics, Faculty of Mathematics and Physics, Charles University, Ke Karlovu 5, 12116 Prague 2, Czech Republic
[3] Department of Inorganic Chemistry, Faculty of Science, Charles University, Hlavova 2030/8, 12843 Prague 2, Czech Republic
[4] Institut Laue-Langevin – The European Neutron Source, 71 avenue des Martyrs, F-38042 Grenoble, France
[5] Department of Physics of Materials, Faculty of Mathematics and Physics, Charles University, Ke Karlovu 5, 12116 Prague 2, Czech Republic

* Corresponding author's e-mail: suhaas96@gmail.com

Supplementary Information

Figure S1: SAXS plot and Guinier-Porod function fit of the colloidal dispersion of the synthesised MAPbBr3 NPLs

Figure S2: Time-resolved ensemble PL decay measurement of the reference toluene solvent and the synthesised $MAPbBr_3$ NPL colloidal dispersion fitted with a single-exponential decay curve

Figure S3: (a) and **(b)** SEM images of the synthesised $MAPbBr_3$ NPLs spin-coated onto a silica wafer captured with a middle in-lens detector for secondary electrons; **(c)** and **(d)** the same SEM images captured with an upper in-lens detector for surface sensitive SE. The images depict the well-isolated NPLs and their layered morphological features

Figure S4: (a) Spectral image of the sample captured on the camera, the vertical yellow box highlights the image of the slit, and the horizontal yellow box highlights the single peak emission spectrum of an individual $MAPbBr_3$ NPL; **(b)** Single peak emission spectrum integrated over 2 lines for a single $MAPbBr_3$ NPL marked in Figure S2(a) with a horizontal yellow box; **(c)** Frequency count histogram depicting the wavelength binning of the singular emission peaks observed from 61 individual $MAPbBr_3$ NPLs

Figure S5: (a) Spectral image of the sample captured on the camera, the vertical yellow box highlights the image of the slit, and the horizontal green boxes (top: light green, bottom: dark green) highlight the double peak emission spectra of 2 individual $MAPbBr_3$ NPLs; **(b)** Double peak emission spectra integrated over 2 lines for 2 single $MAPbBr_3$ NPLs marked in Figure

S3(a) with horizontal green boxes; **(c)** Frequency count histogram depicting the wavelength binning of the double emission peaks observed from 167 individual $MAPbBr_3$ NPLs

Figure S6: (a) Spectral image of the sample captured on the camera, the vertical blue box highlights the image of the slit, and the horizontal blue box highlights the triple peak emission spectrum of an individual $MAPbBr_3$ NPL; **(b)** Triple peak emission spectrum integrated over 3 lines for a single $MAPbBr_3$ NPL marked in Figure S4(a) with a horizontal yellow box; **(c)** Frequency count histogram depicting the wavelength binning of the triple emission peaks observed from 119 individual NPLs

Figure S7: (a) Spectral image of the sample captured on the camera, the vertical orange box highlights the image of the slit, and the horizontal orange box highlights the multi-peak emission spectrum of an individual $MAPbBr_3$ NPL; **(b)** Multi-peak emission spectrum integrated over 3 lines for a single $MAPbBr_3$ NPL marked in Figure S5(a) with a horizontal orange box; **(c)** Frequency count histogram depicting the wavelength binning of the multi-peak emission observed from 134 individual $MAPbBr_3$ NPLs

Figure S8: Frequency count histograms depicting the wavelength binning of the multi-peak PL emission observed from 481 individual $MAPbBr_3$ NPLs, separated by the number of emission peaks observed, i.e., single-, double-, triple- or multi-peak emission of a single particle. The peak counts are normalised against the number of emission peaks in the 440-450 nm wavelength bin for each histogram individually

Figure S9: Emission spectra integrated over the wafer area under the slit across 4 successive spectral image captures, i.e., emission spectra from 4 different populations of $MAPbBr_3$ NPLs that have been continuously laser irradiated for increasing time from the 1^{st} to the 4^{th} capture

Figure S10: AFM images obtained **(a)** 2 hours, **(c)** 48 hours, and **(e)** 430 hours after casting 0.8 μL of synthesised $MAPbBr_3$ NPLs onto a mica substrate; **(b)**, **(d)**, and **(f)** are the size distribution histograms of the respective AFM images

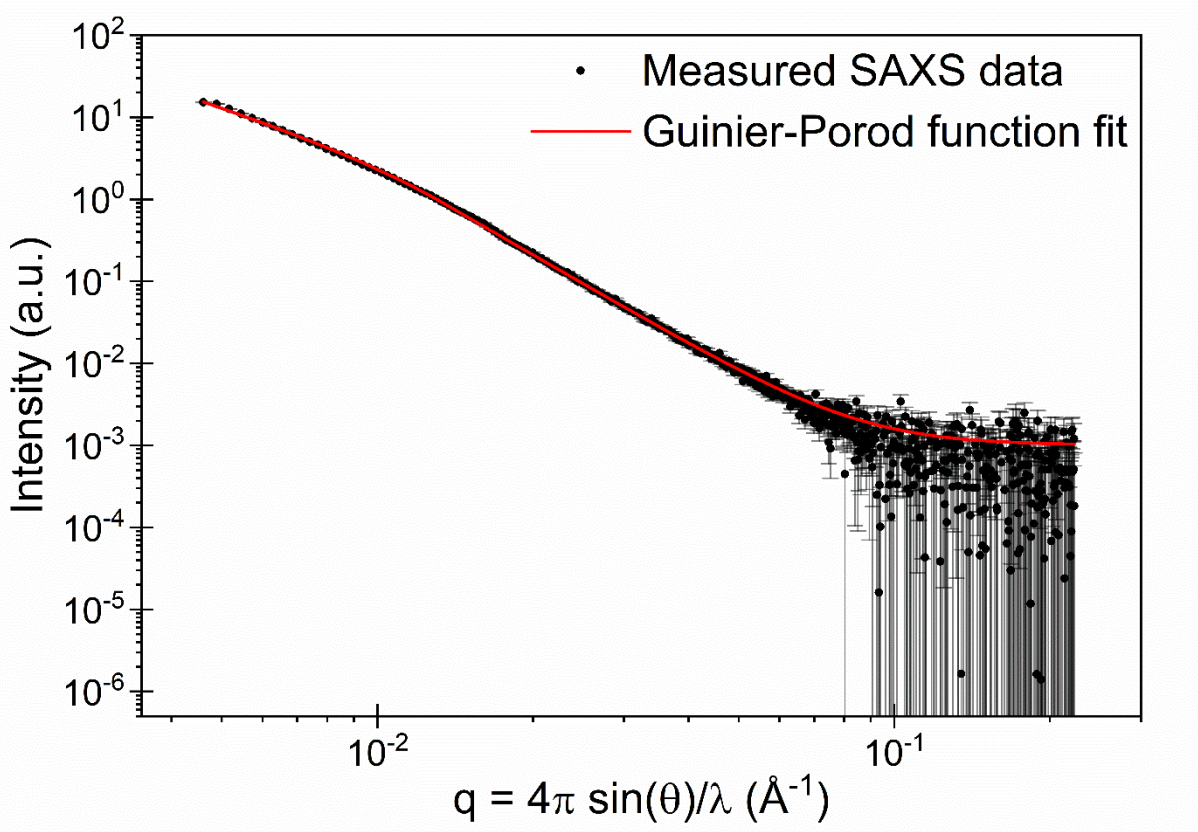

Figure S1: SAXS plot and Guinier-Porod function fit of the colloidal dispersion of the synthesised MAPbBr3 NPLs

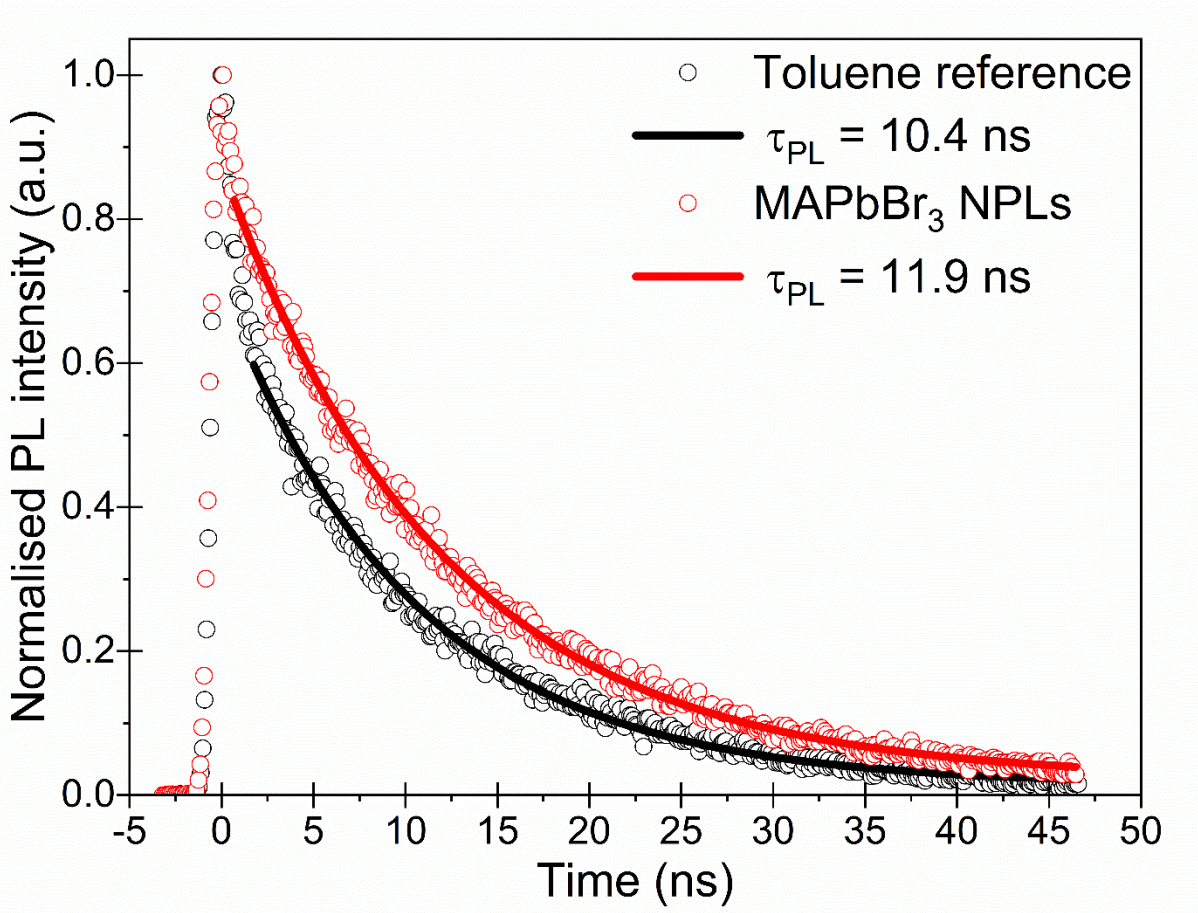

Figure S2: Time-resolved ensemble PL decay measurement of the reference toluene solvent and the synthesised $MAPbBr_3$ NPL colloidal dispersion fitted with a single-exponential decay curve

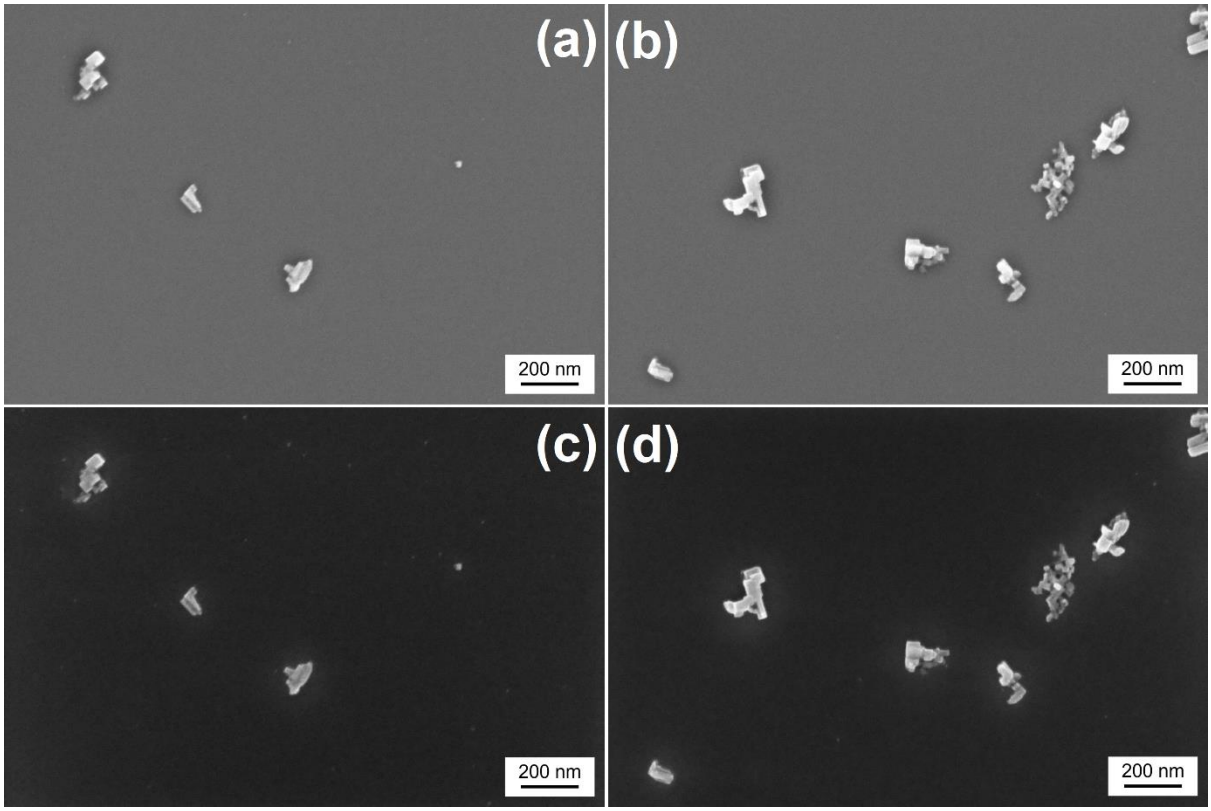

Figure S3: (a) and **(b)** SEM images of the synthesised $MAPbBr_3$ NPLs spin-coated onto a silica wafer captured with a middle in-lens detector for secondary electrons (SE); **(c)** and **(d)** the same SEM images captured with an upper in-lens detector for surface sensitive SE. The images depict the well-isolated NPLs and their layered morphological features

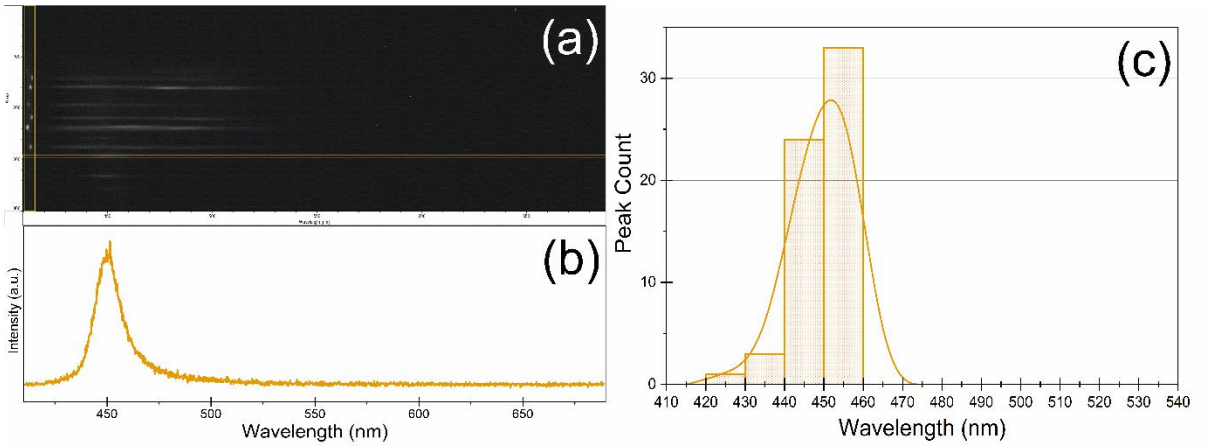

Figure S4: (a) Spectral image of the sample captured on the camera, the vertical yellow box highlights the image of the slit, and the horizontal yellow box highlights the single peak emission spectrum of an individual $MAPbBr_3$ NPL; **(b)** Single peak emission spectrum integrated over 2 lines for a single $MAPbBr_3$ NPL marked in Figure S2(a) with a horizontal

yellow box; **(c)** Frequency count histogram depicting the wavelength binning of the singular emission peaks observed from 61 individual $MAPbBr_3$ NPLs

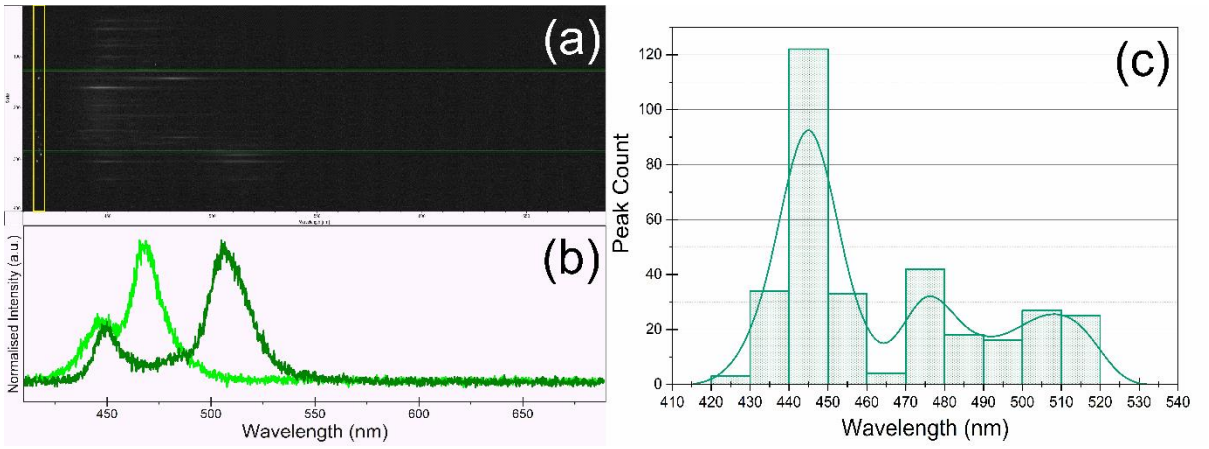

Figure S5: (a) Spectral image of the sample captured on the camera, the vertical yellow box highlights the image of the slit, and the horizontal green boxes (top: light green, bottom: dark green) highlight the double peak emission spectra of 2 individual $MAPbBr_3$ NPLs; **(b)** Double peak emission spectra integrated over 2 lines for 2 single $MAPbBr_3$ NPLs marked in Figure S3(a) with horizontal green boxes; **(c)** Frequency count histogram depicting the wavelength binning of the double emission peaks observed from 167 individual $MAPbBr_3$ NPLs

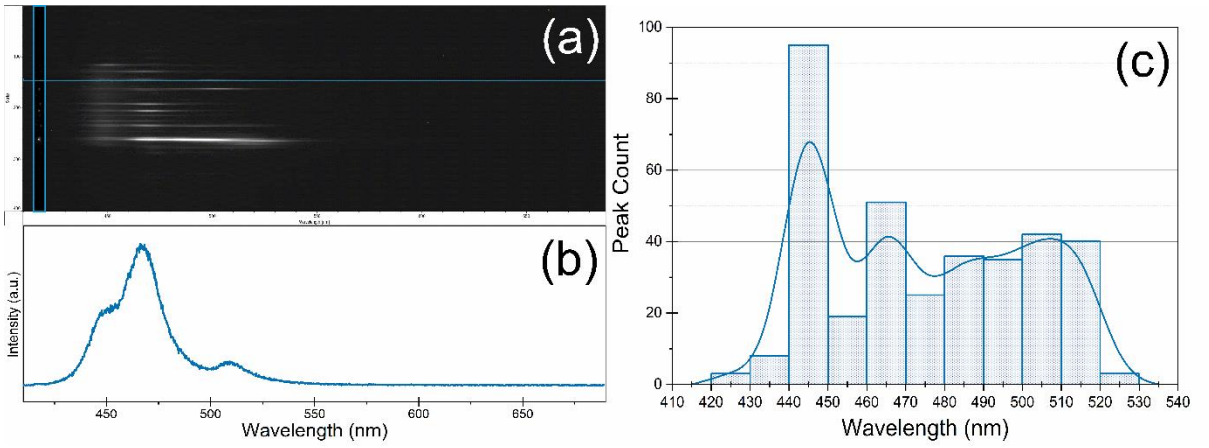

Figure S6: (a) Spectral image of the sample captured on the camera, the vertical blue box highlights the image of the slit, and the horizontal blue box highlights the triple peak emission spectrum of an individual $MAPbBr_3$ NPL; **(b)** Triple peak emission spectrum integrated over 3 lines for a single $MAPbBr_3$ NPL marked in Figure S4(a) with a horizontal yellow box; **(c)**

Frequency count histogram depicting the wavelength binning of the triple emission peaks observed from 119 individual NPLs

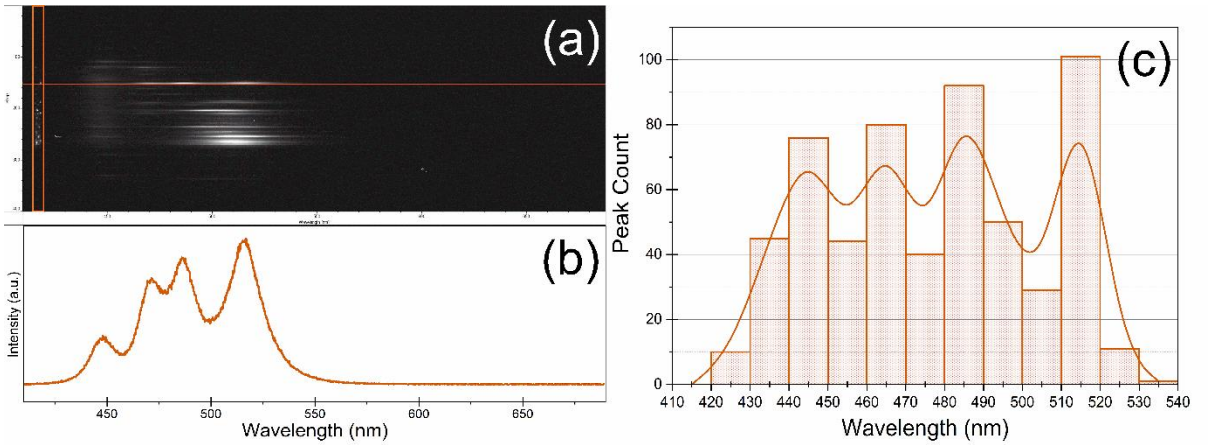

Figure S7: (a) Spectral image of the sample captured on the camera, the vertical orange box highlights the image of the slit, and the horizontal orange box highlights the multi-peak emission spectrum of an individual $MAPbBr_3$ NPL; **(b)** Multi-peak emission spectrum integrated over 3 lines for a single $MAPbBr_3$ NPL marked in Figure S5(a) with a horizontal orange box; **(c)** Frequency count histogram depicting the wavelength binning of the multi-peak emission observed from 134 individual $MAPbBr_3$ NPLs

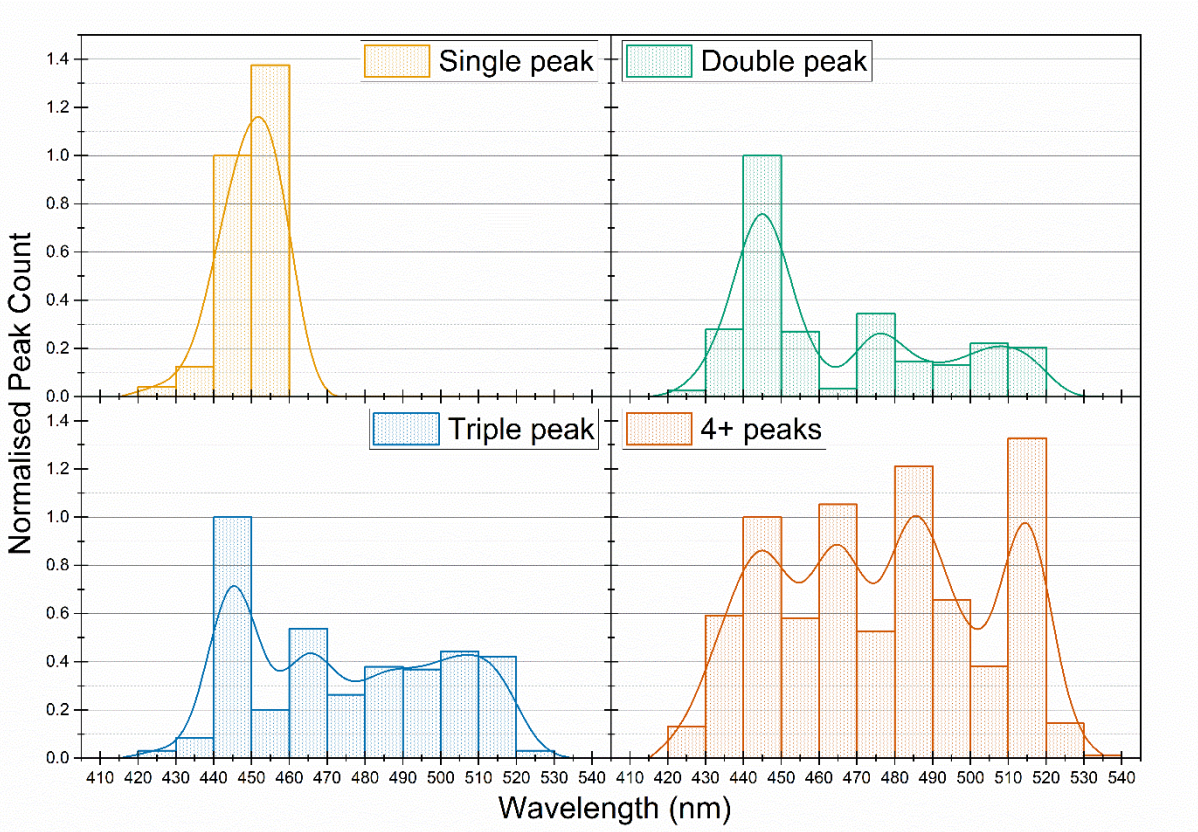

Figure S8: Frequency count histograms depicting the wavelength binning of the multi-peak PL emission observed from 481 individual $MAPbBr_3$ NPLs, separated by the number of emission peaks observed, i.e., single-, double-, triple- or multi-peak emission of a single particle. The peak counts are normalised against the number of emission peaks in the 440-450 nm wavelength bin for each histogram individually

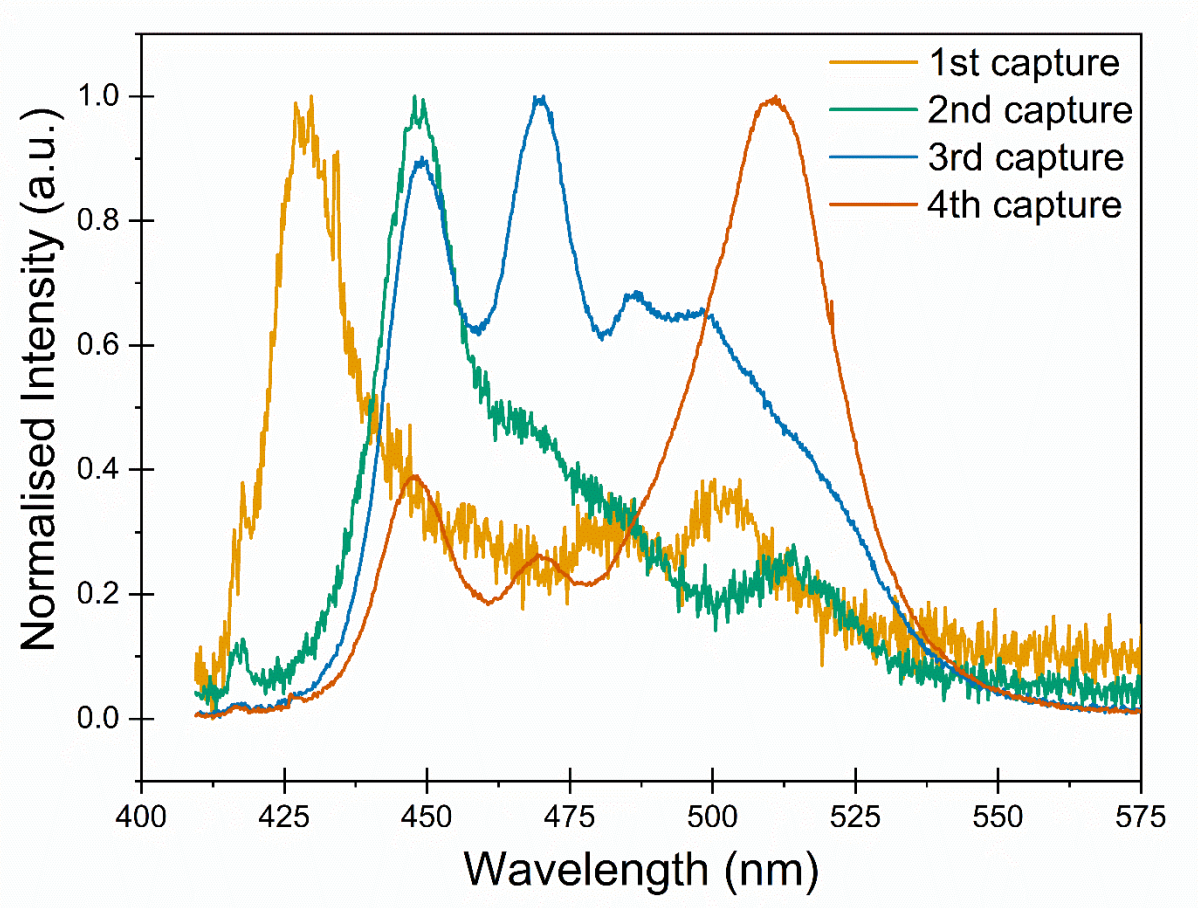

Figure S9: Emission spectra integrated over the wafer area under the slit across 4 successive spectral image captures, i.e., emission spectra from 4 different populations of $MAPbBr_3$ NPLs that have been continuously laser irradiated for increasing time from the 1st to the 4th capture

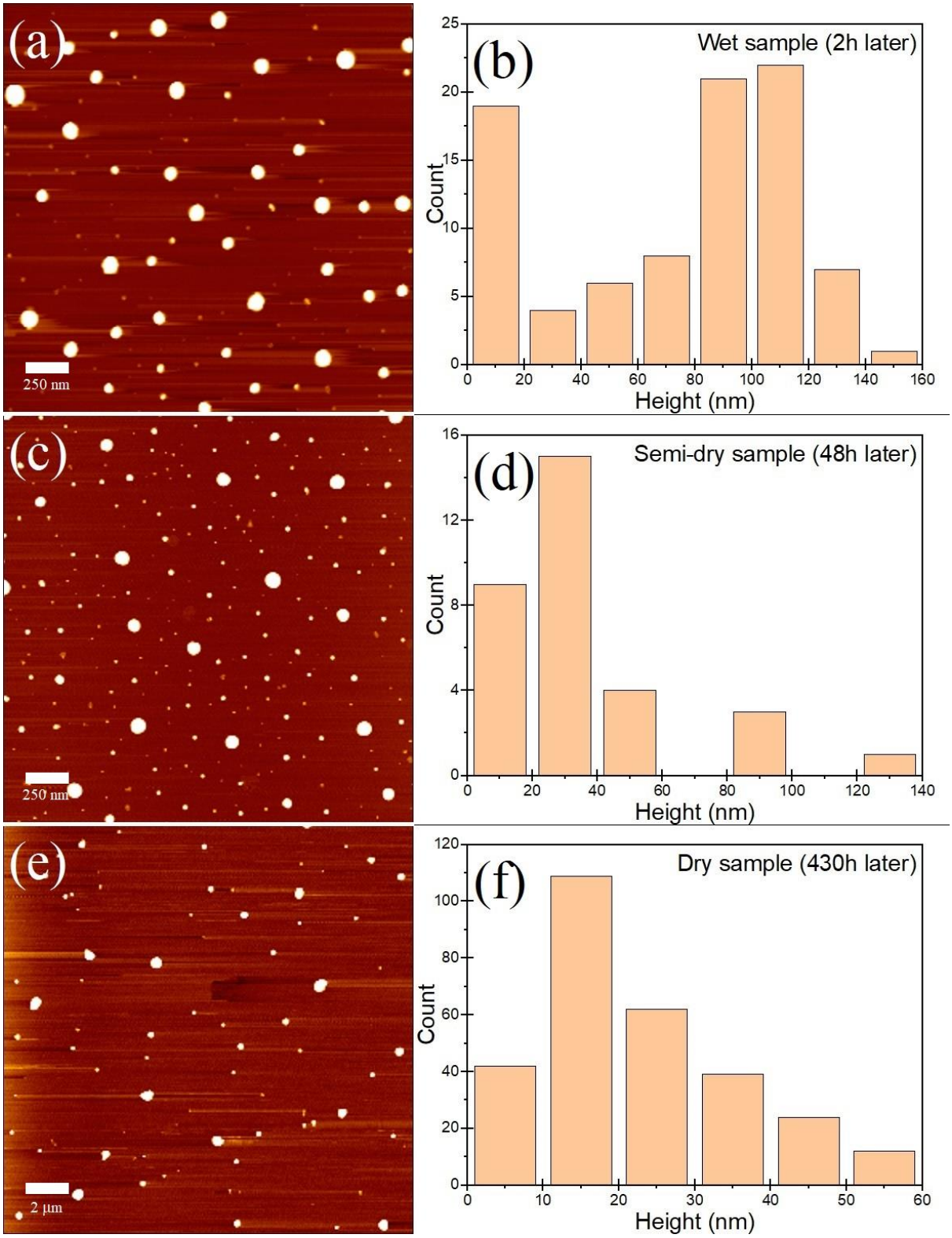

Figure S10: AFM images obtained **(a)** 2 hours, **(c)** 48 hours, and **(e)** 430 hours after casting 0.8 μL of synthesised $MAPbBr_3$ NPLs onto a mica substrate; **(b)**, **(d)**, and **(f)** are the size distribution histograms of the respective AFM images